

Fan the Flame with Water: Current Ignition, Front Propagation and Multiple Steady States in Polymer Electrolyte Membrane Fuel Cells

Jay Benziger

Dept. of Chemical Engineering, Princeton University, Princeton, NJ 08544

DOI 10.1002/aic.12117

Published online November 3, 2009 in Wiley InterScience (www.interscience.wiley.com).

Keywords: fuel cell, energy, polymer electrolyte, water, steady state multiplicity

Introduction

Fuel cells have tantalized engineers for more than a century as efficient devices to directly convert chemical energy to electrical energy. However, fuel cell use has been limited to niche applications, like space vehicles and emergency backup power systems, due to their expensive components and specialized fuel requirements. During the past two decades polymer electrolyte membrane (PEM) fuel cells have attracted the attention of the transportation industry, because they operate at modest temperatures (0–100°C), and do not involve highly corrosive liquids as electrolytes. Although PEM fuel cells are a promising technology they present new design challenges to engineers. This Perspective illustrates how classical chemical reactor engineering can help solve one of the most vexing problems of PEM fuel cells — how to manage water.

PEM fuel cells are coupled chemical reactors where oxidation and reduction reactions are physically separated and coupled by transport of ions and electrons.^{1–4} Hydrogen is adsorbed onto a catalyst surface and is oxidized to protons and electrons at the anode. A chemical potential gradient drives the protons to migrate across the electrolyte. Electrons move through a parallel path in an electronic conductor, where they do useful work. The protons and electrons meet and react with oxygen on a catalyst surface at the cathode.

PEM fuel cells have complex structures that facilitate chemical reaction and heat and mass transport. At the heart of the PEM fuel cell is the membrane-electrode assembly (MEA), a polymer electrolyte membrane coated on both sides with a thin layer of carbon supported Pt catalyst. Nafion is the most common PEM; it is a copolymer of tetrafluoroethylene and a perfluoro alkyl ether terminated with a covalently bonded sulfonic acid.^{5,6} Water absorbs into Nafion solvating

the sulfonic acid groups, swelling the membrane and permitting mobility of the protons.

The catalyst-coated membrane is sandwiched between a porous carbon layer approximately 200–400 μm thick, called the gas diffusion layer (GDL).⁷ The GDL carries the electronic current while permitting the reactant gases to diffuse to the membrane/catalyst interface. The MEA is placed between metal or graphite plates with flow channels (bipolar plates). The flow channels deliver the reactant gases across the MEA, collect and remove the product water and conduct the electronic current.

Water management is essential to efficient PEM fuel cell operation.^{8,9} Proton conductivity in Nafion increases from 10^{-7} to 10^{-1} S-cm as water activity increases from 0 to 1 (relative humidity increasing from 0 to 100%).¹⁰ To achieve the highest proton conductivity and minimize energy losses in the polymer electrolyte, PEM fuel cells have been operated with humidified feeds.^{2,4} However, with humidified feeds, the product water condenses and liquid water can hinder reactant gas transport from the gas-flow channel through the GDL to the membrane/catalyst interface. The brute force engineering solution for PEM fuel cells is to humidify the feeds and operate with high reactant gas flow rates to blow the liquid drops out of the fuel cell; the high-gas-flow results in low-fuel conversion per pass, necessitating recovery and recycle systems.

The flow patterns for the gas-flow channels are generally complex, most often consisting of long serpentine type channels 10–1,000 cm long with cross sections $< 1 \text{ mm}^2$. Liquid water accumulates at various locations in the GDL and the gas-flow channels, resulting in a condition known as flooding. Liquid water can hinder mass transport, locally starving the fuel cell, resulting in variable local current densities and voltages. Understanding the spatiotemporal dynamics of water formation and motion in PEM fuel cells remains a great challenge for fuel-cell engineering, especially when the water production and flow rates change in time as occurs with start-up, shutdown and with variable load.

Recently several groups have developed probes for local current, composition and temperature measurements in

J. Benziger's e-mail address is benziger@princeton.edu.

serpentine flow fields of the fuel-cell test stations,^{11–13} and other groups have used NMR and neutron scattering to map water concentrations in the fuel cell.^{14–18} These studies have observed spatiotemporal changes. However, most studies have been qualitative in nature and there has been limited analysis, either experimental or modeling, of dynamic operation of PEM fuel cells.

Steady-state 1-D (one-dimensional) and 2-D models of transport and reaction in the GDL and MEA of PEM fuel cells have been developed. Excellent reviews of the modeling efforts are available.^{5,19,20} These models have incorporated detailed accounts of the transport and reaction through the various layers of the MEA (the catalyst layer, GDL and membrane). The models have been able to provide a semi-quantitative description of the steady-state current voltage relationship for PEM fuel cells. However, there are many “unknown” parameters in these models that are adjusted to fit the integrated current and voltage of a PEM fuel cell. There have been few data that provide a robust validation of the reactor models.

Characterization of fuel cell operation has focused on the “polarization curve”, where the current through and voltage across an external load are measured while the load impedance (R_L) is varied from zero to infinity. Reaction conditions in a typical serpentine flow channel fuel-cell test station are not well-defined. From the inlet to the outlet the vapor/liquid fractions change, membrane water content changes and compositions at the anode and cathode change, all of which give rise to current and voltage variations throughout the fuel cell. Furthermore, the dynamic response of the fuel cell is complicated by multiple time constants: ~ 1 s for changes in gas composition; $\sim 10^3$ s for liquid water drop formation; $> 10^5$ s for water absorption in the polymer membrane. Polarization curves associated with complex flow fields cannot unravel the fuel-cell dynamics to test and validate models.

Chemical Engineers have employed simplified chemical reactors to elucidate the physics coupling chemical reaction, mass transport and heat transport in complex systems. The model reactors are a crucial step in model validation between the bench-top experiment and commercial scale. Electrochemists have used idealized rotating disc electrode systems to elucidate the electrode kinetics, but the application of simplified flow geometries to fuel cells has been overlooked. To obtain data that can identify the fundamental physics of dynamic PEM operation and validate mathematical models of fuel cells, data from simpler, better defined systems is needed.

A chapter has been borrowed from the “Chemical Reactor Engineering Playbook” to elucidate the chemistry and physics of how water is transported in PEM fuel cells. Model PEM fuel cells have recently been built based on simplified flow geometries: (1) a differential or “stirred-tank reactor” fuel cell, and (2) a single channel parallel flow or “plug-flow reactor” fuel cell. The well-defined flow geometries associated with these model reactors connect specific reaction conditions of composition and temperature with local voltage and current density. These model systems are ideal to understand both steady state and dynamic operation and the simplified model reactors can serve as building blocks to predict the performance of large-scale fuel cells with complex flow configurations.

Stirred-Tank Reactor PEM Fuel Cell

A stirred-tank reactor PEM fuel cell was created by replacing the long thin flow channels by an open plenum.²¹ “Uniform” composition is achieved by diffusive mixing when the characteristic diffusion time in the gas plenums is less than the residence time for flow through the plenum, as given by Eq. 1

$$\tau_{diffusion} = \frac{\{A_{mem}h_{plenum}\}^{2/3}}{D_{gas}} > \tau_r = \frac{\{A_{mem}h_{plenum}\}}{Q_{gas}} \quad (1)$$

A simple STR PEM fuel cell constructed at Princeton has an MEA area of ~ 2 cm² and the height of the plenums was ~ 0.25 cm. For typical gas-phase diffusivities of ~ 1 cm²/s, diffusive mixing was adequate to assure uniform compositions for flow rates < 0.8 cm³/s, corresponding to maximum current densities of ~ 3 A/cm².

With uniform composition in the gas plenums the STR PEM fuel cell is 1-D; the only gradients are transverse across the membrane; the anode and cathode effluent compositions are the same as those inside the fuel cell. Current, voltage, temperature and anode and cathode relative humidities measurements were logged as a function of time providing all the necessary information to relate composition to current density at a given cell temperature.

The STR PEM fuel cell was first employed to identify the critical requirements for humidification for the fuel cell to operate. It has been asserted that “extra humidification of the reactant gases is essential in PEM fuel cells operating above about 60°C. This has been confirmed by the general experience of PEM fuel cell users”^{4,22} The Department of Energy has had a substantial program to identify new membrane materials that could operate at temperatures above 100°C with low-relative humidity.²³ So what are the critical constraints for operating a PEM fuel cell with dry feeds?

To operate the STR PEM fuel cell with dry feeds the membrane was dried by flowing dry N₂ through the fuel cell for several hours at 80°C at open circuit ($R_L = \infty$); then the fuel cell was switched on — the load resistance was set and reactant feeds turned on, H₂ at the anode and O₂ at the cathode. When the membrane’s initial state was totally dry no measurable current was observed. The STR PEM fuel cell was then tested with dry feeds, but prehydrating the membrane to change the initial condition.

The results in Figure 1 show the current as a function of time starting from different initial states of hydration (given as mass of water absorbed per unit area of the MEA). Below a critical level of initial hydration the fuel cell current extinguished over time. When the initial hydration was above the critical level the current ignited and leveled off at a high steady-state value.²⁴ After the current ignited, the relative humidities at the anode and the cathode both increased and leveled out to steady-state values that are $> 80\%$ RH.²⁵ Ignition of the fuel-cell current with dry feeds has been demonstrated for temperatures of 25–130°C.^{26,27} Clearly the fuel cell operated autohumidified, and extra humidification of the reactant gases was not essential.

How does the fuel-cell current ignite? The key is the water balance. At steady-state water produced by reaction in the fuel

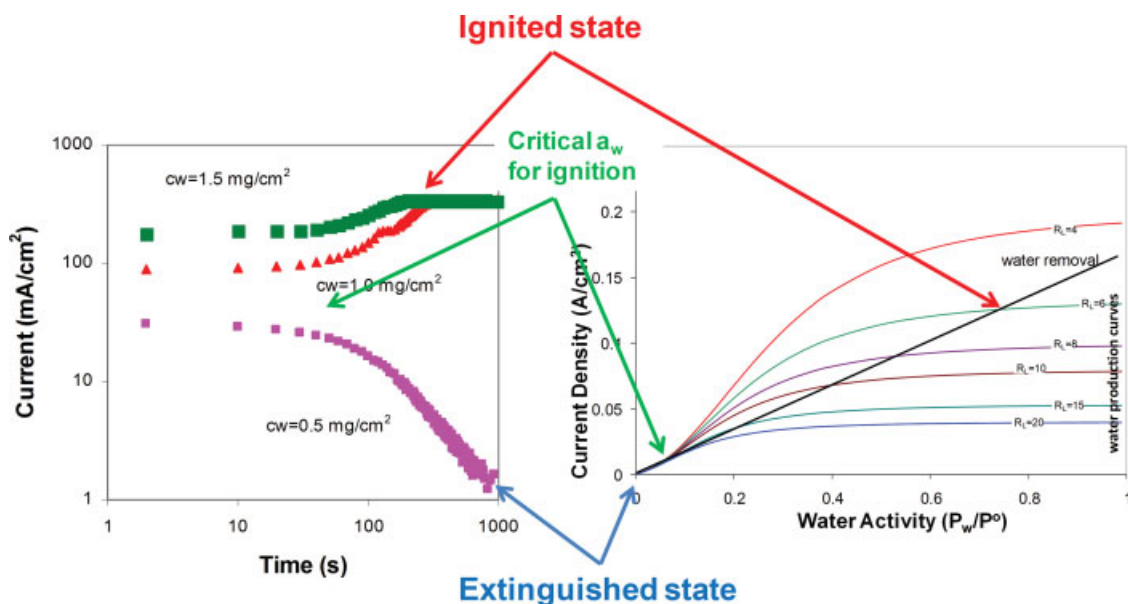


Figure 1. Current Ignition of an STR PEM fuel cell.

Left: Critical initial water content for current ignition in a STR PEM fuel cell reactor. Different amounts of water were injected into the fuel cell and allowed to equilibrate with the membrane for 1 h. The fuel cell was then started up with dry feeds, anode: $8 \text{ cm}^3 \text{ H}_2/\text{min}$ and cathode: $4 \text{ cm}^3 \text{ O}_2/\text{min}$, and with a load impedance of 2Ω . The current through the load was recorded as a function of time (note the log-log scale associated with the large change in current and the long-time scale for ignition). Right: Mass balance showing water generation and water removal from a STR PEM fuel cell as functions of membrane water activity (assuming the membrane water activity is equilibrated with the vapor at both the anode and cathode). Three steady states exist: an extinguished state near $a_w = 0$ with near zero current, an ignited state at high a_w with high current, and an unstable steady-state circa $a_w \sim 0.1$ corresponding to the critical condition for current ignition.

cell must be balanced by water removed by gas convection through the cell, as described by Eq. 2^{21,24,28,29}

Water produced by reaction = Water removed by convection

$$\frac{I}{2F} = \frac{Q_A P_w^0}{RT} a_w^{\text{anode}} + \frac{Q_C P_w^0}{RT} a_w^{\text{cathode}} \quad (2)$$

Water removal is given by the flow rates at the anode and cathode multiplied by the respective water activities. Water production is equal to half the proton current (one water is produced for every two protons that cross the membrane). The current is given by Ohm's law as the voltage across the fuel cell divided by the sum of the membrane resistance and the load resistance. The voltage depends on the difference of hydrogen activity at the anode and cathode, for illustrative purposes only the thermodynamic potential is considered for the voltage. The resistance of the Nafion membrane was found to increase exponentially with water activity.¹⁰

The fuel-cell current as a function of temperature, composition and load resistance is given by Eq. 3. (The fuel-cell literature often presents data assuming current is an independent parameter. This is misleading—the load resistance is the independent parameter that the operator manipulates. Most testing employs a galvanostat that manipulates the load resistance to deliver a desired current.) The membrane resistance decreases exponentially with water activity, so that the current (water production) increases sigmoidally with water activity. Water

removal increases linearly with water activity as shown in the graph on the right side of Figure 1

$$I = \frac{V}{R_{\text{membrane}} + R_{\text{Load}}} = \frac{V_o + \frac{RT}{2F} \ln \left\{ \frac{p_{\text{H}}^{\text{anode}}}{(p_{\text{O}}^{\text{cathode}})^{1/2} p_{\text{w}}^{\text{cathode}}} \right\}}{R_o \exp \left[-14 (a_w^{\text{membrane}})^{0.2} \right] + R_{\text{Load}}} \quad (3)$$

Water production and removal curves intersect at three points corresponding to steady states; an extinguished steady state with near zero current, an ignited steady state at high current, and an intermediate unstable steady state corresponding to the critical condition for ignition. The critical initial membrane water content for ignition is the unstable steady state at $a_w \sim 0.1$. Equations 2 and 3 reveal that the current in PEM fuel cells can be extinguished by increasing flow rates, increasing temperature or increasing the load resistance. The dynamics of current ignition in PEM fuel cells are slow ($\sim 10^3 \text{ s}$ based on Figure 1). Current ignition requires water absorption into the polymer membrane. Water absorption is governed by diffusion and the dynamics of polymer swelling which have long-time constants.^{30–33}

Hogarth and Benziger demonstrated that the STR PEM fuel cell can be ignited by a “water match”²⁷ a single injection of water into an extinguished fuel cell can ignite the current. The current will ignite within seconds, but the time to reach the final steady state can take more than 10^5 s (several days)

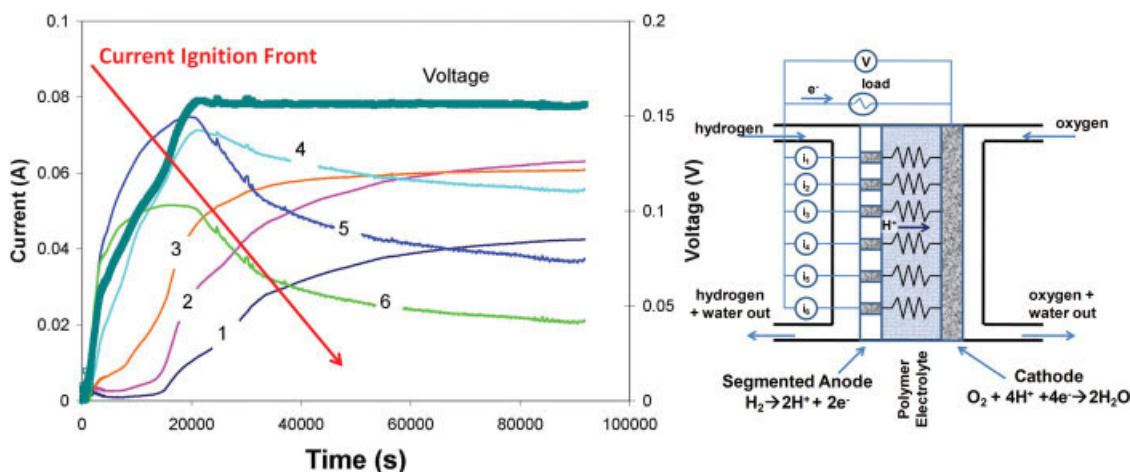


Figure 2. Ignition and extinction front propagation in a PFC PEM fuel cell.

Front propagation results from a balance of convection of water in the gas-flow channels and diffusion of water in the membrane. The schematic to the right illustrates the segmented anode employed to look at the current ignition front propagation. The careful reader will notice that the PFC resembles a “tanks-in-series” model for flow, but the electrical circuit has resistances in parallel.

because of the slow equilibration of water absorption by Nafion.

The STR PEM fuel cell displays multiple steady states analogous to those in other well mixed systems where exponential feedback between a reaction product and reaction rate ignites the reaction. The autothermal reactor, or flame is the classic example from Reaction Engineering text books. Even though PEM fuel cells have been around for more than 40 years, the simple concept of fuel cell current ignition by water and the critical conditions for autohumidified operation had been completely missed because of the complexity of the prevailing fuel-cell flow field designs. Steady-state multiplicity has been identified in solid-oxide fuel cells (SOFC) (where oxygen anions are conducted across a zirconia electrolyte), which have displayed current ignition. Ignition in SOFCs results from an exponential increase in ion conductivity with temperature in zirconia, giving rise to autothermal operation.^{34–36}

Parallel Flow Channel Fuel Cell

The plug-flow reactor is the second most common model reactor; it introduces the complexity of axial spatial gradients. The fuel-cell analog of the plug-flow reactor was created by having two parallel flow channels (PFC) for the anode and cathode, separated by the membrane electrode assembly.³⁷ To probe axial gradients in the current density, the anode was segmented into six sections, permitting the local current density along the flow channel to be measured.

The PFC fuel-cell current was ignited by various methods: a single water injection, reducing the inlet flow rates, reducing the cell temperature or reducing the load impedance. The current evolves in both time and space after ignition of the PFC fuel cell. Current ignition with cocurrent flow is illustrated in Figure 2.^{37,38} The current first ignites at the outlet (position 6), and then a current density wave moves from the outlet toward the inlet (position 1). The physics of ignition and front

propagation results from the interplay of convection and diffusion. Initially the water formed is convected downstream in the gas flow. Water accumulates in the membrane at the outlet. If the water accumulation reaches the critical water activity, the current will ignite at the outlet. After ignition, a water concentration gradient is established in the membrane, and product water will start diffusing upstream. The diffusion will cause the ignition front to propagate toward the inlets.

Ignition, extinction and front propagation are all well-known phenomena in the context of exothermic reactions where positive feedback between heat generation, heat removal by convection and heat conduction produce qualitatively similar behavior. PEM fuel cells display the same characteristics, but in this case they arise from production and transport of water. The exponential increase of proton conductivity with water activity in the polymer plays the same role in PEM fuel cells as the Arrhenius exponential temperature dependence of the reaction rate for exothermic reactions. Model reactors have illuminated how PEM fuel cells are analogous to classical chemical reactors.

The conditions for autohumidified operation are dramatically different for the STR and PFC fuel cells. Hogarth and Benziger demonstrated that a STR PEM fuel cell with a standard Nafion membrane could operate with a current density of 1 A/cm² at 0.6 V with dry feeds at a temperature of 80°C, and a total pressure of 1 bar. Increasing the total pressure to 3 bar increased the maximum temperature for operating with dry feeds to 130°C.^{26,27} Kimball et al. showed that the PFC fuel cell achieved maximum current densities <0.1 A/cm² at 0.5 V and 80°C.³⁹ Flow field and mixing have a tremendous impact on the operation. This may seem obvious to chemical engineers, but was overlooked by the chemists and mechanical engineers building fuel cells.

The importance of different flow patterns is reflected in the Peclet number for different reactor types. ($Pe = (\text{diffusive transport}/\text{convective transport})$). The STR PEM fuel cell was designed to maximize diffusive mixing, hence, a large Pe

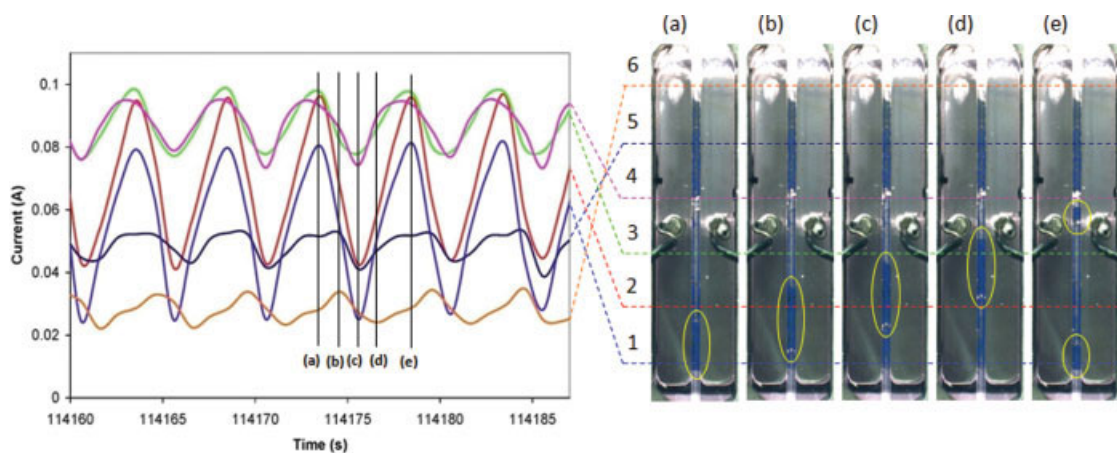


Figure 3. Correlation of liquid water motion in the cathode flow channel with local current density in the PFC fuel cell.

The fuel cell was positioned with the flow channels vertical and the gas flows were cocurrent and against to gravity. (a) Slugs form between segments 1 and 2, (b) slugs begin to move up the channel against gravity and stationary slug stuck at the top of the channel is pushed up, (c) slugs continue to be pushed up, but slows down, (d) slugs start to become smaller while continuing to be pushed up the channel, and (e) slugs stop moving up the channel while the water falls back toward the inlet, creating another slug at the same location where the first one formed. The flow channels in the PFC are 1.6 mm wide and 64 mm long. Typical water slugs were ~15 mm long.

number. The long thin flow channels for the PFC fuel cell and serpentine fuel cells promote high-gas velocities leading to small Pe numbers. The ratio of the Pe numbers for the STR and PFC (or serpentine) fuel cells, assuming the same reactant flow per area of MEA, is given by Eq. 4. The serpentine flow design has smaller Pe number than the STR design — hence, the mixing of dry feeds with water produced in the fuel cell is dramatically reduced. The enhanced backmixing of the STR design permits the water in the fuel cell to mix with the feeds to facilitate autohumidification. Even for relatively small cells, mixing with serpentine flow is not sufficient to operate with dry feeds

$$\frac{Pe_{serpentine,anode}}{Pe_{STR,anode}} = \frac{(D/v_{serpentine}L_{serpentine})}{(D/v_{STR}L_{STR})} = \frac{\left(\frac{Q}{hA^{1/2}_{membrane}}\right)\left(\frac{1}{A^{1/2}_{membrane}}\right)}{\left(\frac{Q}{hw_{channel}}\right)\left(\frac{A_{membrane}}{w_{channel}}\right)} = \frac{w_{channel}^2}{A_{membrane}} \quad (4)$$

Two-Phase Flow in PEM Fuel Cells

The previous section focused on the critical water content for fuel-cell ignition (start-up) and dynamics of ignition, where all the water was convected from the fuel cell as a vapor. Steady-state PEM fuel-cell operation at high-power produces more water than can be convected out as water vapor. Liquid water accumulates in the PEM fuel cell and must be removed. The parallel flow channel fuel cell was adapted to examine two-phase flow in PEM fuel cells. The anode and cathode were fitted into polycarbonate to permit visual observation of the gas-flow channels. Flow visualization with a segmented anode

permitted correlation of local current density measurements with liquid flow in the gas-flow channel.

Direct flow observations showed that liquid does not flood the pores of the GDL as had been commonly assumed,⁴⁰ but liquid water emerges from the gas-diffusion layer into the cathode flow channel in only a few locations, corresponding to the largest pores of the GDL.^{14,41} The drops grow in the flow channel until the forces on the drop exceeds the strength of drop adhesion to the liquid in the GDL pore, then drops break free, coalesce and form slugs in the flow channel. Water slugs on the GDL surface hinder gas flow from the flow channel to the membrane/catalyst interface and locally shut down the current because of reactant starvation.³⁹ Under such conditions the orientation of the PFC fuel cell relative to gravity has a profound effect on the cell operation; gravity can assist with water removal (flow channel vertical with gas flow in the direction of gravity), be neutral (flow channel horizontal), or have a negative impact (flow channel vertical with gas-flow opposing gravity).^{37,39} Figure 3 is an example of the correlated video images and local current measurements when the gas flow was counter to gravity. Very regular periodic current density fluctuations occurred. Water drops fall due to gravity, forming slugs near the gas inlet. When the slugs grew large enough, the gas flow can no longer bypass the water slug, and the upstream section of the fuel cell was starved for reactant causing the current density to drop in that part of the fuel cell. Gas pressure built up below the water slug and eventually pushed the slug up the flow channel; after the slug was pushed out of the flow channel the local current density was restored to a high value.

The simple PFC reactor permits observation of how liquid drops and slugs move causing current density variations that depend on operating parameters and fuel-cell construction. These data and complementary data for liquid/gas flow in microfluidics channels are advancing our understanding of the

Table 1. Comparison of Autothermal Reactors and Autohumidified PEM Fuel Cells

Autothermal Reactor	Autohumidified PEM Fuel Cell
Balance of Heat Generation and Heat Removal	Balance of Water Generation and Water Removal
Temperature ignition and extinction	Current ignition and extinction
Increasing flow extinguishes flame	Increasing flow extinguished current
Flame fronts propagation controlled by heat conduction	Current density fronts propagation controlled by water diffusion

performance of complex flow channel systems employed in commercial fuel cells.

Conclusions

Reactor design can play an important a role in improving fuel-cell performance. Classical simplified model chemical reactors have helped elucidate how water is formed and transported in PEM fuel cells.

The results from the stirred-tank reactor fuel cell showed classical steady-state multiplicity with ignition and extinction of the current, resulting from positive feedback between the water product and the proton conductivity in the polymer electrolyte membrane. The simplified 2-D parallel flow channel fuel cell demonstrated the existence of propagating current density fronts, just like flame fronts in exothermic reactions. Table 1 summarizes the analogy between autohumidified PEM fuel cells and autothermal reactors. These analogies provide a conceptual framework to think about water management in the engineering design of PEM fuel cells.

These simplified fuel-cell reactors have elucidated some of the complexities of fuel-cell operation associated with commercial fuel cells. The simplified parallel flow channel fuel cell is beginning to unravel the physics of drop and slug formation and movement, especially the correlation between liquid water motion in the gas-flow channels and local current density fluctuations. The simple geometry of the PFC fuel cell also permitted clear observations of the relative importance of gravity to the shear forces from gas flow in moving liquid through the fuel cell.

The initial observations and discovery of multiple steady states in PEM fuel cells were totally unexpected. In hindsight they appear obvious, but the complex flow fields associated with PEM fuel-cell systems obscured the phenomena for more than 25 years. Experience from the past six years has demonstrated the importance of developing simplified model systems to identify the key physics associated with the reaction and transport in PEM fuel cells. We cannot overstate the importance of practicing the fundamental approach taught in reaction engineering — start by understanding the simplified reactors — and build more complex systems based on a solid physical understanding of the simple systems. Recent results suggest that better engineering designs of PEM fuel-cell reactors may be more important to the commercial success of fuel cells than developing bet-

ter membranes and catalysts, which has been the focus of the DOE road map.

Acknowledgments

I owe a great deal of thanks to a large number of undergraduate students and graduate students who humored me in initiating this work. Special thanks go to: Joel Moxley who built the first STR fuel cell as his senior thesis project and demonstrated the existence of multiple steady states, and Joanne Chia and Erin Kimball who developed the Parallel Flow Channel fuel cells and demonstrated current density front propagation, and the correlations of liquid water movement and local current densities. I am especially indebted to Ioannis Kevrekidis for collaborating with the dynamic modeling and his continual encouragement. Finally, we thank the NSF for providing financial support.

Notation

$a_w = P_w/P_w^0$	= water activity
A_{mem}	= active area of membrane electrode assembly
D_{gas}	= gas-phase diffusivity
F	= Faraday's constant
h	= height of gas-flow channel or gas plenum
I	= current
l_{mem}	= thickness of polymer electrolyte membrane
L	= length of gas-flow channel
P	= pressure in fuel cell
Pe	= Peclet number (Dwh/QL)
Q	= volumetric gas-flow rate
R	= gas constant
R_L	= load resistance
R_{mem}	= membrane resistance
T	= temperature
V	= fuel-cell voltage
V_0	= standard state fuel-cell voltage
w	= width of gas-flow channel
τ_r	= residence time for flow through the fuel cell
τ_D	= characteristic diffusion time in the gas-flow channel

Literature Cited

1. Blomen LJM, Mugerwa MN. Fuel Cell Systems. New York: Plenum; 1993:614.
2. Barbir F. PEM Fuel Cells: Theory and Practice. Dorf RC, ed. Academic Press Sustainable World Series. Burlington, MA: Elsevier Academic Press; 2005.
3. EG&G Services P, Inc. Fuel Cell Handbook. Morgantown, WV: US Department of Energy; 2000:312.
4. Larminie J, Dicks A. Fuel Cell Systems Explained. 2nd ed. New York: Wiley; 2003.
5. Thampan T, Malhotra S, Zhang JX, Datta R. PEM fuel cell as a membrane reactor. *Catal Today*. 2001;67(1–3): 15–32.
6. Vielstich W, Lamb A, Gasteiger H. Handbook of Fuel Cells. Indianapolis: Wiley; 2003:1.
7. Mathias M, Roth J, Fleming J, Lehnert W. Diffusion media materials and characterization. In: Vielstich W, Gasteiger H, Lamm A, eds. Handbook of Fuel Cells - Fundamentals, Technology and Applications. London: John Wiley & Sons; 2003:3.

8. Costamagna P, Srinivasan S. Quantum jumps in the PEMFC science and technology from the 1960s to the year 2000 Part II. Engineering, technology development and application aspects. *J Power Sources*. 2001;102(1–2): 253–269.
9. Yu XC, Zhou B, Sobiesiak A. Water and thermal management for Ballard PEM fuel cell stack. *J Power Sources*. 2005;147(1–2):184–195.
10. Yang C, Srinivasan S, Bocarsly AB, Tulyani S, Benziger JB: A comparison of physical properties and fuel cell performance of Nafion and zirconium phosphate/Nafion composite membranes. *J Membr Sci*. 2004; 237(1–2):145–161.
11. Hogarth WHJ, Steiner J, Benziger JB, Hakenjos A. Spatially-resolved current and impedance analysis of a stirred tank reactor and serpentine fuel cell flow-field at low relative humidity. *J Power Sources*. 2007;164(2): 464–471.
12. Mench MM, Wang CYH. An in situ method for determination of current distribution in PEM fuel cells applied to a direct methanol fuel cell. *J Electrochem Soc*. 2003;150(1):A79–A85.
13. Mench MM, Dong QL, Wang CY. In situ water distribution measurements in a polymer electrolyte fuel cell. *J Power Sources*. 2003;124(1):90–98.
14. Bazylak A. Liquid water visualization in PEM fuel cells: A review. *Int J Hydrogen Energy*. 2009;34(9):3845–3857.
15. Bedet J, Maranzana G, Leclerc S, Mutzenhardt P, Canet D, Lottin O, Moyne C, Stemmelen D. Magnetic resonance imaging of water distribution and production in a 6 cm(2) PEMFC under operation. *Int J Hydrogen Energy*. 2008;33(12):3146–3149.
16. Dunbar Z, Masel RI: Quantitative MRI study of water distribution during operation of a PEM fuel cell using Teflon (R) flow fields. *J Power Sources*. 2007;171(2):678–687.
17. Weber AZ, Hickner MA. Modeling and high-resolution-imaging studies of water-content profiles in a polymer-electrolyte-fuel-cell membrane-electrode assembly. *Electrochim Acta*. 2008;53(26):7668–7674.
18. Siegel JB, McKay DA, Stefanopoulou AG, Hussey DS, Jacobson DL. Measurement of liquid water accumulation in a PEMFC with dead-ended anode. *J Electrochem Soc*. 2008;155(11):B1168–B1178.
19. Weber AZ, Newman J. Modeling transport in polymer-electrolyte fuel cells. *Chem Rev*. 2004;104:4679–4726.
20. Wang CY. Fundamental models for fuel cell engineering. *Chem Rev*. 2004;104:4727–4766.
21. Benziger J, Chia E, Karnas E, Moxley J, Teuscher C, Kevrekidis IG. The stirred tank reactor polymer electrolyte membrane fuel cell. *AIChE J*. 2004;50(8):1889–1900.
22. Buchi FN, Srinivasan S. Operating proton exchange membrane fuel cells without external humidification of the reactant gases - Fundamental aspects. *J Electrochem Soc*. 1997;144(8):2767–2772.
23. Hydrogen, Fuel Cells & Infrastructure Technologies Program Multi-Year Research, Development and Demonstration Plan Planned program activities for 2005–2015. US Department of Energy; 2007. http://www1.eere.energy.gov/hydrogenandfuelcells/pdfs/htwg_rd_plan.pdf
24. Moxley JF, Tulyani S, Benziger JB. Steady-state multiplicity in the autohumidification polymer electrolyte membrane fuel cell. *Chem Eng Sci*. 2003;58(20):4705–4708.
25. Benziger J, Chia E, Moxley JF, Kevrekidis IG. The dynamic response of PEM fuel cells to changes in load. *Chem Eng Sci*. 2005;60(6):1743–1759.
26. Hogarth WHJ, Benziger JB: Operation of polymer electrolyte membrane fuel cells with dry feeds: Design and operating strategies. *J Power Sources*. 2006;159:968–978.
27. Hogarth WHJ, Benziger JB. Dynamics of autohumidified PEM fuel cell operation. *J Electrochem Soc*. 2006; 153(11):A2139–A2146.
28. Chia ESJ, Benziger JB, Kevrekidis IG: Water balance and multiplicity in a polymer electrolyte membrane fuel cell. *AIChE J*. 2004;50(9):2320–2324.
29. Benziger J. Reactor Dynamics of PEM Fuel Cells. Device and Materials Modeling in Pem Fuel Cells. *Topics in Applied Physics: Springer*. 2009;113:91–122.
30. Satterfield MB, Benziger JB. Non-fickian water vapor sorption dynamics by nafion membranes. *J Phys Chem B*. 2008;112(12):3693–3704.
31. Satterfield MB, Benziger JB: Viscoelastic properties of nafion at elevated temperature and humidity. *J Polym Sci Part B-Polym Phys*. 2009;47(1):11–24.
32. Majsztrik PW, Bocarsly AB, Benziger JB: Viscoelastic response of nafion. effects of temperature and hydration on tensile creep. *Macromolecules*. 2008;41(24):9849–9862.
33. Majsztrik PW, Satterfield MB, Benziger J, Bocarsly AB. Water sorption, desorption and transport in Nafion membranes. *J Membr Sci*. 2007;301:93–106.
34. Bhattacharyya D, Rengaswamy R. A review of solid oxide fuel cell (sofc) dynamic models. *Ind Eng Chem Res*. 2009;48(13):6068–6086.
35. Debenedetti PG, Vayenas CG. Steady-state analysis of high-temperature fuel-cells. *Chem Eng Sci*. 1983;38(11): 1817–1829.
36. Mangold M, Krasnyk M, Sundmacher K. Theoretical investigation of steady state multiplicities in solid oxide fuel cells. *J Appl Electrochem*. 2006;36(3):265–275.
37. Benziger J, Chia JE, Kimball E, Kevrekidis IG. Reaction dynamics in a parallel flow channel PEM fuel cell. *J Electrochem Soc*. 2007;154(8):B835–B844.
38. Benziger JB, Chia JE-S, DeDecker Y, Kevrekidis IG. Ignition front propagation in polymer electrolyte membrane fuel cells. *J Phys Chem C*. 2007;111(5):2330–2334.
39. Kimball E, Whitaker T, Kevrekidis YG, Benziger JB. Drops, slugs, and flooding in polymer electrolyte membrane fuel cells. *AIChE J*. 2008;54(5):1313–1332.
40. Pasaogullari U, Wang CY. Liquid water transport in gas diffusion layer of polymer electrolyte fuel cells. *J Electrochem Soc*. 2004;151(3):A399–A406.
41. Benziger J, Nehlsen J, Blackwell D, Brennan T, Itescu J. Water flow in the gas diffusion layer of pem fuel cells. *J Membr Sci*. 2005;261:98–106.

